

# Structure determination of the nonlinear hydrocarbon chains $C_9H_3$ and $C_{11}H_3$ by deuterium labeling

Dongfeng Zhao (赵东锋),<sup>1,a)</sup> Mohammad Ali Haddad,<sup>1</sup> Harold Linnartz,<sup>1,2</sup> and Wim Ubachs<sup>1</sup>

<sup>1</sup>*Institute for Lasers, Life, and Biophotonics, VU University Amsterdam, De Boelelaan 1081, NL 1081 HV Amsterdam, The Netherlands*

<sup>2</sup>*Raymond and Beverly Sackler Laboratory for Astrophysics, Leiden University, P.O. Box 9513, NL 2300 RA Leiden, The Netherlands*

(Received 10 May 2011; accepted 27 July 2011; published online 19 August 2011)

A systematic deuterium labeling experiment is presented that aims at an unambiguous determination of the geometrical ground state structure of the  $C_9H_3$  and  $C_{11}H_3$  hydrocarbon chains. Cavity ring-down spectroscopy and special plasma expansions constituting C/H, C/D, and C/H/D are used to record optical transitions of both species and their (partially) deuterated equivalents in the 19 000  $cm^{-1}$  region. The number of observed bands, the quantitative determination of isotopic shifts, and supporting calculations show that the observed  $C_9H_3$  and  $C_{11}H_3$  spectra originate from  $HC_4(CH)C_4H$  and  $HC_4[C(C_2H)]C_4H$  species with  $C_{2v}$  symmetry. This result illustrates the potential of deuterium labeling as a useful approach to characterize the molecular structure of nonlinear hydrocarbon chains.

© 2011 American Institute of Physics. [doi:10.1063/1.3626151]

## I. INTRODUCTION

Unsaturated hydrocarbon chains of the form  $C_nH_m$  (+/-) (typically with  $m \leq n$ ), both linear and nonlinear, have been topic of many experimental and theoretical studies. These reactive species are found as important intermediates in combustion and flames,<sup>1,2</sup> in plasma environments,<sup>3</sup> and in dense interstellar clouds, where many hydrocarbons have been unambiguously identified.<sup>4-6</sup> Studies dedicated to the structural determination of these transient intermediates have made it possible to improve models to characterize combustion processes or to quantify reaction pathways of relevance to interstellar chemistry. In the past three decades, microwave and infrared studies have provided accurate molecular constants yielding structure determinations for a large number of unsaturated hydrocarbon chain species.<sup>7,8</sup> More recently high resolution optical work in combination with high level *ab initio* results have extended these studies to electronic transitions.<sup>9,10</sup> This is important, particularly for those systems, where microwave and infrared data are not available. However, for many nonlinear carbon chain radicals exhibiting small rotational constants or lifetime broadened transitions, rotational resolution cannot be obtained and consequently unambiguous structure determinations are not possible. In such cases isotopic labeling provides an additional tool to derive structural information.

In this contribution the ground state structures of two trihydrogenated carbon chain radicals,  $C_9H_3$  and  $C_{11}H_3$ , are conclusively determined from gas phase optical spectra and deuterium (D) labeling. Their optical spectra have been previously reported,<sup>11,12</sup> but molecular structures were not unambiguously determined because of a lack of rotationally re-

solved transitions in the experimental spectra.  $C_7H_3$ , a smaller molecule with similar molecular form, was identified as a three-member ring chain with  $C_s$  symmetry,<sup>13</sup> but density functional theory (DFT) calculations<sup>14</sup> predicted that the open chain isomers of  $HC_4(CH)C_4H$  and  $HC_4[C(C_2H)]C_4H$  with  $C_{2v}$  symmetry (shown in Fig. 1) are the most likely carriers of experimental spectra previously recorded for  $C_9H_3$  and  $C_{11}H_3$ , respectively. For  $C_9H_3$  this is consistent with the outcome of a recent study<sup>15</sup> in which the *K*-stack structure could be resolved.

## II. EXPERIMENTAL AND THEORETICAL METHODS

The  $C_9H_3$  and  $C_{11}H_3$  spectra are recorded by pulsed cavity ring-down spectroscopy through a supersonically expanding hydrocarbon plasma.<sup>16</sup> The plasma source employs a modified pinhole discharge nozzle which has been described in detail previously (see Ref. 15 for details). An acetylene/helium gas mixture is expanded with a backing pressure of  $\sim 7$  bar into a high vacuum chamber that is pumped by a roots blower system with a total capacity of 1000  $m^3/h$ . The typical chamber pressure during jet operation amounts to 0.03 mbar. Three gas mixtures, 0.5%  $C_2H_2/He$ , 0.3%  $C_2D_2/He$ , and (0.2%  $C_2H_2 + 0.2\% C_2D_2/He$ ), are used in the present experiment to create C/H, C/D, and C/H/D plasma jets, respectively. A high voltage pulse ( $\sim 300 \mu s$  and  $-1000 V$ ) is applied to the electrodes of the discharge nozzle coinciding with a gas pulse of 1 ms duration which is generated by a pulsed valve (General Valve, Series 9) mounted to the vacuum chamber. The plasma expansion perpendicularly crosses the optical axis of a 58 cm long optical cavity,  $\sim 7$  mm downstream. This cavity consists of two plano-concave mirrors (Research Electro-Optics, reflectivity  $> 99.995\%$  in the wavelength range 515–550 nm) that are mounted on high precision alignment tools. Cavity ring-down events are obtained

<sup>a)</sup> Author to whom correspondence should be addressed. Electronic mail: d.zhao@vu.nl.

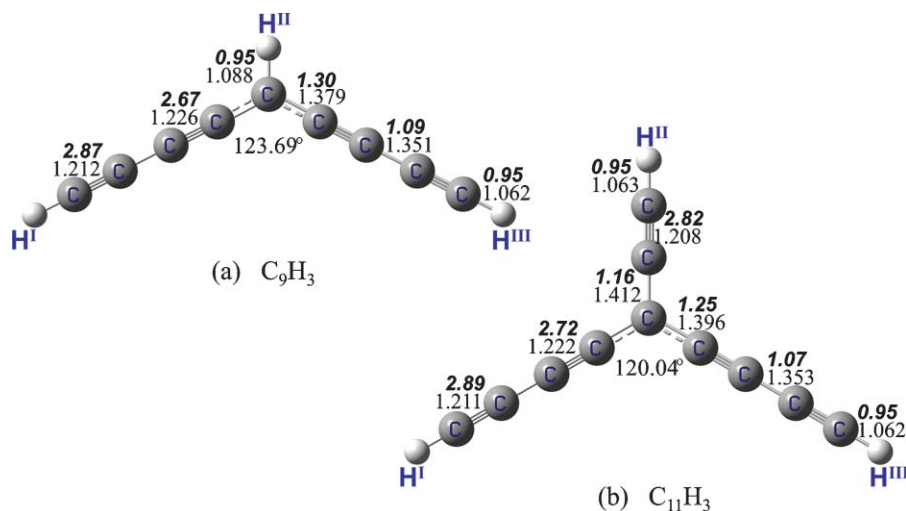


FIG. 1. The molecular structure of (a)  $C_9H_3$  and (b)  $C_{11}H_3$ . The bond lengths (in Angstrom) and the angles of the bend  $C_{2v}$  structures, calculated at the DFT-B3LYP/6–311G\*\* level, are indicated by regular numbers. The calculated bond indices of the two radicals are indicated by bold numbers.

by injecting a fraction of the laser pulse into the high-finesse optical cavity. Light leaking out of the cavity is detected by a photomultiplier tube and typical ring-down times amount to 60–80  $\mu$ s. The setup is operated at 10 Hz, determined by the repetition rate of a tripled Nd:YAG laser (355 nm) that is used to pump a dye laser (Sirah, Cobra-Stretch, bandwidth  $\sim 0.04$   $cm^{-1}$ ). A trigger scheme allows optimizing the timing of the ring-down event with respect to the discharge pulse. The absolute laser frequency is calibrated with a precision better than 0.02  $cm^{-1}$  using an  $I_2$  absorption reference spectrum that is recorded simultaneously.

The analysis of the experimental data is supported by a set of additional DFT calculations. The structural optimization of stationary points and vibrational frequencies in the ground state are calculated by the DFT-B3LYP (Ref. 17) method. Complete active space multiconfiguration SCF calculations<sup>18</sup> with 7 electrons and 8 orbitals in the active space (CASSCF (7, 8)) are performed for the derived molecular structures to characterize the role of the active molecular orbitals involved in the observed electronic spectra. For this, the 6–311G (*d, p*) basis set is used. All these calculations are performed using the GAUSSIAN 03 software package.<sup>19</sup>

### III. RESULTS AND ANALYSIS

#### A. Experimental spectra

The absorption spectra of  $C_9H_3$  and  $C_{11}H_3$  recorded through a C/H plasma are shown in Figs. 2(a) and 3(a). Based on previous studies involving mass-spectrometric detection,<sup>11,12</sup> these spectra can be unambiguously assigned to electronic transitions of  $C_9H_3$  and  $C_{11}H_3$ . Here, similar absorption bands are observed in a C/D plasma (shown in Figs. 2(b) and 3(b)) at blueshifts of  $\sim 70$   $cm^{-1}$ , corresponding to isotopically shifted  $C_9D_3$  and  $C_{11}D_3$ . In a mixed C/H/D plasma all these bands are observed as well (though weaker), and in addition several new bands appear (shown in Figs. 2(c) and 3(c)). The latter exhibit similar band contours and comparable intensities, and are ascribed to partially deuterated (D) isotopologues.

#### B. Structure determination of $C_9H_3$

Rotational constants for  $C_9H_3$  have been previously estimated as  $A'' \approx 0.215$   $cm^{-1}$ , and  $B'' \approx C'' \approx 0.0159$   $cm^{-1}$  from a spectral contour fit of an *a*-type transition, reflecting the nonlinear structure of this molecule.<sup>15</sup> For large molecules such as  $C_9H_3$ , the difference between rotational constants of different isotopologues is generally small. The DFT calculations confirm that the rotational constants of different isotopologues are very comparable (see Table I), and within the uncertainties of the empirical contour fit from the experimental spectrum of  $C_9H_3$ . The experimentally derived rotational constants of  $C_9H_3$  are therefore also used in the spectral simulations of the individual absorption bands of the different isotopologues in order to derive the band origin positions of the recorded optical transitions.

In total twelve bands attributed to six D-isotopologues of  $C_9H_3$  are obtained from spectral simulations (Fig. 2(c)), which are assigned to two transition types (Table II): the  $0_0^0$  electronic origin band transitions and vibronic transitions involving excitation of a low-frequency vibration ( $\nu \sim 38$   $cm^{-1}$ ) in the upper electronic state. The intensity ratio of the six isotopologue bands is quantitatively determined to be  $\sim 1:1:2:2:1:1$  from measurement of a 50%/50% H/D mixture in the C/H/D plasma (Fig. 2). The number of observed D-isotopologues and their intensity ratio, subsequently allows for a conclusion on the symmetry of the molecule and the position of the three hydrogen atoms. This is explained below.

We label the three hydrogen positions in the geometric structure of  $C_nH_3$  as  $H^I$ ,  $H^{II}$ , and  $H^{III}$ , and use  $H^IH^{II}H^{III}$  as an overall label. We discriminate three possible cases:

- (1) The three hydrogen atoms are non-interchangeable, corresponding to three fundamental H/D isotopic shifts of  $\Delta^I$ ,  $\Delta^{II}$  and  $\Delta^{III}$ . In this case, eight D-isotopologues should be observed: HHH, DHH, HDH, HHD, DDH, DHD, HDD, and DDD, with indicative isotopic shifts of  $\sim 0$ ,  $\Delta^I$ ,  $\Delta^{II}$ ,  $\Delta^{III}$ ,  $\Delta^I + \Delta^{II}$ ,  $\Delta^I + \Delta^{III}$ ,  $\Delta^{II} + \Delta^{III}$ ,  $\Delta^I + \Delta^{II} + \Delta^{III}$ . In a plasma with equal amounts of H and D, these eight species will have approximately

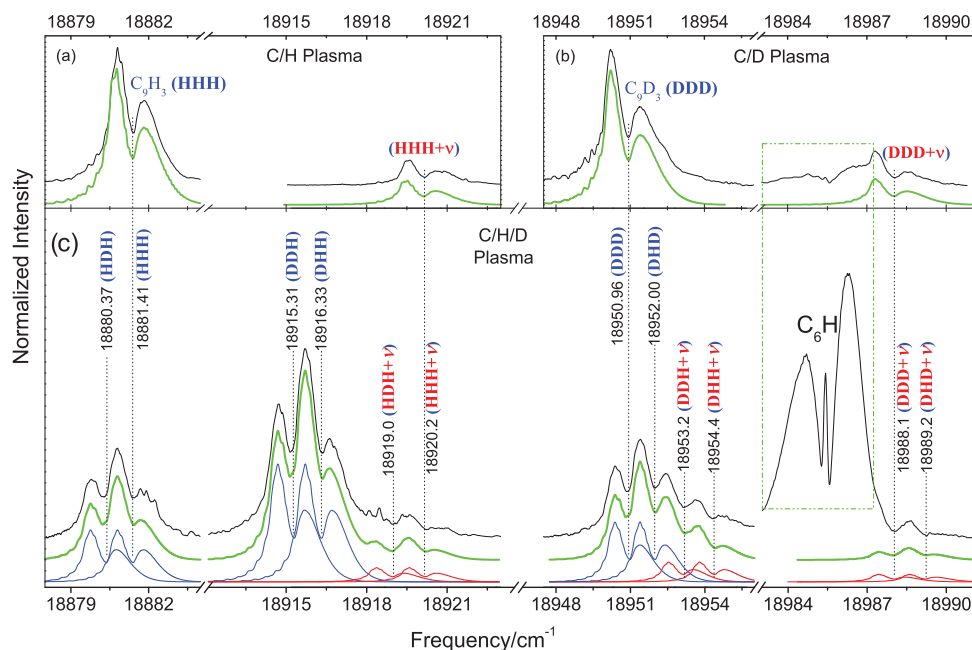


FIG. 2. Experimentally observed spectra (upper black lines) of C<sub>9</sub>H<sub>3</sub> and its D-isotopologues recorded through: (a) C/H, (b) C/D, and (c) mixed C/H/D plasma. The simulated spectra are shown by bold green lines in each panel. In panel (c), the individual simulations of the observed  $\alpha$ -type bands are shown: blue lines indicate the  $0_0^0$  transitions and red lines vibronic bands, respectively. The vertical dotted lines indicate the band origins of the  $0_0^0$  transitions for the D-substituted species (identified in blue) and the vibronic bands (identified in red). The absorption at  $\sim 18985$  cm<sup>-1</sup> in panels (b) and (c) is due to the C<sub>6</sub>H radical. (See Ref. 20).

the same abundance, i.e., their absorbance should be comparable.

- (2) Two hydrogens are at symmetrical positions, e.g., H<sup>I</sup> and H<sup>III</sup> due to a plane of symmetry or a C<sub>2</sub> axis. The two unique hydrogen positions correspond to two fundamental H/D isotopic shifts of  $\Delta^{III}$  and  $\Delta^{II}$ . In this case, the isotopologues DHH and DDH are identical to HHD and

HDD, respectively. Thus, six D-isotopologues should be observed: HHH, HDH, DHH/HHD, DDH/HDD, DHD, and DDD, with indicative isotopic shifts of  $\sim 0$ ,  $\Delta^{II}$ ,  $\Delta^{III}$ ,  $\Delta^{III} + \Delta^{II}$ ,  $2\Delta^{III}$ ,  $2\Delta^{III} + \Delta^{II}$ , and a statistical intensity ratio of  $\sim 1:1:2:2:1:1$ , respectively.

- (3) The three hydrogens are fully symmetrical within a C<sub>3v</sub> or D<sub>3h</sub> molecular point group, i.e., there exists only one

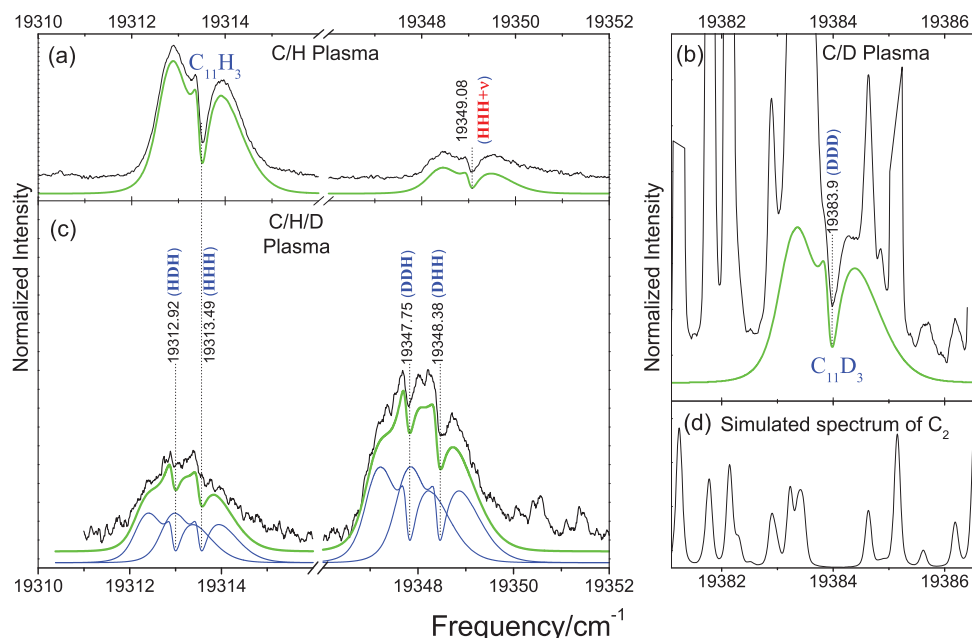


FIG. 3. Experimentally observed spectra (upper black lines) of C<sub>11</sub>H<sub>3</sub> and its D-isotopologues recorded through (a) C/H, (b) C/D, and (c) C/H/D plasma. The simulated spectra are represented by bold green lines. In panel (c), the individual simulations of the observed  $\alpha$ -type bands are shown by blue lines. The spectrum in panel (d) consists of simulated rotational lines of C<sub>2</sub> which overlap with the electronic origin band of C<sub>11</sub>D<sub>3</sub>.

TABLE I. Calculated rotational constants and low-frequency bending vibrations (in  $\text{cm}^{-1}$ ) for all D-isotopologues of  $\text{C}_9\text{H}_3$  and  $\text{C}_{11}\text{H}_3$  at the B3LYP/6-311G\*\* level.

Isotopologues <sup>a</sup>	$\text{C}_9(\text{H}^{\text{I}}\text{H}^{\text{II}}\text{H}^{\text{III}})$				$\text{C}_{11}(\text{H}^{\text{I}}\text{H}^{\text{II}}\text{H}^{\text{III}})$			
	A	B	C	$\nu^{\text{b}}$	A	B	C	$\nu^{\text{b}}$
HDH	0.2101	0.0164	0.0152	42.26	0.0449	0.0171	0.0124	38.78
HHH <sup>c</sup>	0.2268	0.0164	0.0153	42.43	0.0475	0.0171	0.0126	38.86
DDH/HDD	0.2044	0.0159	0.0148	41.41	0.0443	0.0166	0.0121	38.02
DHH/HHD	0.2203	0.0159	0.0148	41.58	0.0468	0.0166	0.0123	38.09
DDD	0.1988	0.0155	0.0143	40.58	0.0437	0.0162	0.0118	37.27
DHD	0.2140	0.0155	0.0144	40.73	0.0462	0.0162	0.0120	37.33

<sup>a</sup>D-isotopologue formulas are indicated by the permutation  $\text{H}^{\text{I}}\text{H}^{\text{II}}\text{H}^{\text{III}}$ .

<sup>b</sup>Scaled by a factor of 0.968. (Ref. 21).

<sup>c</sup>Values used for spectral simulations of all isotopologues.

unique hydrogen position in the molecular structure. In this case, four D-isotopologues are expected: HHH, DHH, DDH, and DDD, with indicative isotopic shifts of  $\sim 0$ ,  $\Delta$ ,  $2\Delta$ ,  $3\Delta$ , and a statistical intensity ratio of  $\sim 1:3:3:1$ , respectively.

These arguments only hold when H- and D-substitutions at different molecular sites are energetically comparable, i.e., when the number of observed D-isotopologues of a trihydride and their statistical abundances in a reactive plasma are determined by molecular symmetry and unique (i.e., non-interchangeable) hydrogen positions in its geometric structure. Because of the high electronic temperature in a helium plasma, reactive intermediates are always formed very fast. In local thermodynamic equilibrium, therefore, it is assumed that the production probabilities of (partially) deuterated and hydrogenated hydrocarbon chain radicals are approximately the same.

A comparison with the experimental results, presented in Fig. 2, shows that neither the simplest case of a  $C_1$  molecular point group (with eight expected D-isotopologues) nor a point group of the highest possible symmetry,  $C_{3v}$  or  $D_{3h}$  (with three equivalent H/D positions) apply. Instead the six different ob-

served D-isotopologues must arise from two hydrogen atoms in symmetrical positions in  $\text{C}_9\text{H}_3$  due to a plane of symmetry or a  $C_2$  axis in its geometric structure. The observed intensity ratio is fully consistent with the statistically expected one.

In the following we define for  $\text{C}_9\text{H}_3$  that  $\text{H}^{\text{I}}$  and  $\text{H}^{\text{III}}$  act as the two interchangeable H-atoms. From the observed isotopic shifts and intensity ratios, the spectral assignments of the six observed isotopologues (indicated by the permutation  $\text{H}^{\text{I}}\text{H}^{\text{II}}\text{H}^{\text{III}}$ ) can be obtained (see Fig. 2(c) and Table II). Values for the two fundamental H/D isotopic shifts are determined as  $+34.9 \text{ cm}^{-1}$  ( $\Delta^{\text{I/III}}$ ) and  $-1.0 \text{ cm}^{-1}$  ( $\Delta^{\text{II}}$ ).

In our previous work,<sup>15</sup> we predicted from the observation of a partially resolved rotational spectrum that the most likely symmetry of  $\text{C}_9\text{H}_3$  is  $C_2$  or  $C_{2v}$ , which is consistent with the D-labeling results found here. Obviously, the observation of the number and intensity ratio of different D-isotopologues is unambiguous, and more conclusive than the partially resolved rotational progression previously observed for a series of coinciding rotational transitions.

In Ref. 14, the molecular structures, rotational constants, and vertical electronic transition energy for 15 different  $\text{C}_9\text{H}_3$  isomeric structures have been calculated by DFT. Eight structures have  $C_{2v}$  symmetry. Convolving the electronic

TABLE II. The spectral assignment and isotopic shift (all values in  $\text{cm}^{-1}$ ) of the observed isotopologues of  $\text{C}_9\text{H}_3$  and  $\text{C}_{11}\text{H}_3$ .

Isotopologues $\text{C}_n(\text{H}^{\text{I}}\text{H}^{\text{II}}\text{H}^{\text{III}})$	Origin bands			Vibronic bands			
	$T_0$	$\Delta^{\text{a}}$		$T_v$	$\nu^{\text{b}}$	$\Delta\nu_{\text{obs.}}^{\text{a}}$	$\Delta\nu_{\text{calc.}}^{\text{a,c}}$
$\text{C}_9(\text{HDH})$	18880.37(5)	-1.04(6)	$\Delta^{\text{II}}$	18919.0(1)	38.6(1)	-0.2(1)	-0.17
$\text{C}_9(\text{HHH})$	18881.41(2)	0		18920.21(3)	38.80(5)	0	0
$\text{C}_9(\text{DDH/HDD})$	18915.31(5)	+33.90(6)		18953.2(1)	37.8(1)	-1.0(1)	-1.02
$\text{C}_9(\text{DHH/HHD})$	18916.33(5)	+34.92(6)	$\Delta^{\text{I/III}}$	18954.4(1)	38.1(1)	-0.7(1)	-0.86
$\text{C}_9(\text{DDD})$	18950.96(2)	+69.55(3)		18988.05(5)	37.1(1)	-1.7(1)	-1.85
$\text{C}_9(\text{DHD})$	18952.00(5)	+70.59(6)		18989.2(1)	37.2(1)	-1.6(1)	-1.70
$\text{C}_{11}(\text{HDH})$	19312.92(5)	-0.6(1)	$\Delta^{\text{II}}$				
$\text{C}_{11}(\text{HHH})$	19313.49(3)	0		19349.08(3)	35.6(1)		
$\text{C}_{11}(\text{DDH/HDD})$	19347.75(5)	+34.3(1)					
$\text{C}_{11}(\text{DHH/HHD})$	19348.38(5)	+34.9(1)	$\Delta^{\text{I/III}}$				
$\text{C}_{11}(\text{DDD})$	19383.9(1) <sup>d</sup>	+70.4(1)					
$\text{C}_{11}(\text{DHD})$	-	-					

<sup>a</sup> $\Delta$  denotes the isotopic shift with respect to the main isotopologue  $\text{C}_n(\text{HHH})$ .

<sup>b</sup>Vibrational frequency in the upper electronic state:  $\nu = T_v - T_0$ .

<sup>c</sup>Calculated H/D isotopic shift for the lowest bending vibration at the B3LYP/6-311G\*\* level. (See also Table I).

<sup>d</sup>Blended with  $C_2$  absorption lines. (See Fig. 3(b)).

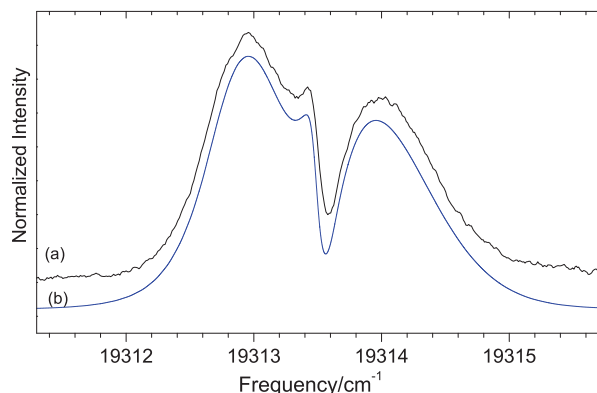


FIG. 4. The electronic origin band spectrum of C<sub>11</sub>H<sub>3</sub>. Trace (a): P- and R-branch contour resolved experimental spectrum; (b): simulated spectrum by an *a*-type transition (with a Gaussian linewidth of  $\sim 0.07$  cm<sup>-1</sup> and rotational temperature of  $\sim 11$  K) from an empirical contour fitting.

transition energy and indicative rotational constants derived from the experimental spectra, only the HC<sub>4</sub>(CH)C<sub>4</sub>H with C<sub>2v</sub> symmetry (shown in Fig. 1(a)) exhibits both a  $1^2A_2 - X^2B_1$  electronic transition (*a*-type) with comparable vertical excitation energy and a set of matching rotational constants. For this specific structure, extended calculations have been performed on the H/D shifts of the low-frequency vibration ( $\Delta\nu$ ) at the B3LYP/6-311G\*\* level. The results are summarized in Tables I and II. As shown in Table II, the calculated values agree well with the experimentally determined values. From this we conclude that the structure of the observed C<sub>9</sub>H<sub>3</sub> is H<sup>(I)</sup>C<sub>4</sub>(CH<sup>(III)</sup>)C<sub>4</sub>H<sup>(III)</sup>.

### C. Structure determination of C<sub>11</sub>H<sub>3</sub>

The  $0_0^0$  electronic origin band transition and the vibronic transition involving excitation of a low-frequency vibration ( $\nu \sim 36$  cm<sup>-1</sup>) in the upper electronic state of C<sub>11</sub>H<sub>3</sub> are clearly observed in the C/H plasma following a similar pattern as for the C<sub>9</sub>H<sub>3</sub> case (Fig. 3(a)). Both of the two bands comprise of unresolved P- and R-branch profiles, separated by a relatively weak Q-branch contour. The *K*-stack structure is not resolved. A rotational contour fit using an *a*-type transition in a nonlinear molecule is applied to the electronic origin band spectrum of C<sub>11</sub>H<sub>3</sub>, as shown in Fig. 4. This yields indicative values of the molecular constants:  $A' \approx 0.05$  cm<sup>-1</sup>,  $B' \approx C' \approx 0.015$  cm<sup>-1</sup>, and  $\Delta(A - (B + C)/2) \approx 0.01$  cm<sup>-1</sup>. These values are substantially smaller than for C<sub>9</sub>H<sub>3</sub>. The experimentally derived C<sub>11</sub>H<sub>3</sub> rotational constants are accurate enough to be used in the spectral simulations of the individual absorption bands of the different D-isotopologues.

As shown in the panels (b) and (c) of Fig. 3, only the electronic origin band transition of the D-isotopologues of C<sub>11</sub>H<sub>3</sub> can be seen in C/D and C/H/D plasma. The electronic origin band of C<sub>11</sub>D<sub>3</sub> is found to coincide with overlapping C<sub>2</sub> absorption lines. Origin band positions are derived from a contour fit, using the approximate rotational constants derived for C<sub>11</sub>H<sub>3</sub>, yielding the values as summarized in Table II. The simulated spectra are included in Fig. 3 as well.

The number of isotopic bands, their relative intensities and the observed H/D isotopic shifts is consistent with a

molecular C<sub>11</sub>H<sub>3</sub> structure with two unique hydrogen positions, i.e., the carrier of the observed C<sub>11</sub>H<sub>3</sub> spectrum has a C<sub>2</sub> or C<sub>2v</sub> symmetry as well. The corresponding values of the two fundamental H/D isotopic shifts are deduced as  $+34.9$  cm<sup>-1</sup> ( $\Delta^{III}$ ) and  $-0.6$  cm<sup>-1</sup> ( $\Delta^{II}$ ), respectively. These values are close to the C<sub>9</sub>H<sub>3</sub> ones. The nearly identical value for  $\Delta^{III}$  in C<sub>9</sub>H<sub>3</sub> and C<sub>11</sub>H<sub>3</sub> indicates a likely similarity between their geometric structures, namely, a similar substructure containing H<sup>I</sup> and H<sup>III</sup>. This means that C<sub>11</sub>H<sub>3</sub> is as C<sub>9</sub>H<sub>3</sub> but with a C<sub>2</sub>H<sup>(III)</sup> group substituting the H<sup>(III)</sup> atom, i.e., HC<sub>4</sub>[C(C<sub>2</sub>H)]C<sub>4</sub>H (Fig. 1(b)). The rotational constants, the low-frequency vibration, and the vertical electronic transition energy of this structure predicted by DFT calculations (see Ref. 14, as well as Table I) are in reasonable agreement with the experimentally derived values. CASSCF calculations show that the  $1^2A_2 - X^2B_1$  electronic transition (*a*-type) of this structure involves very similar electronic configuration and excitation scheme as in C<sub>9</sub>H<sub>3</sub> (see the panels (a) and (b) of Fig. 5). The similarity of the HC<sub>4</sub>C<sup>\*</sup>C<sub>4</sub>H substructure and the involved electronic excitation should result in an approximately identical value of the H/D isotopic shift  $\Delta^{III}$  between C<sub>9</sub>H<sub>3</sub> and C<sub>11</sub>H<sub>3</sub>, which is confirmed by our experimental observations.

It should be noted that two of the other C<sub>11</sub>H<sub>3</sub> isomeric structures listed in Ref. 14 (labeled as B6 and B11) also have a C<sub>2v</sub> symmetry and can be described by a set of rotational constants that is close to the values derived here. However, the low-frequency vibrations and the vertical electronic transition energies of these structures as predicted by DFT calculations (see Ref. 14) deviate substantially from the experimentally derived values. Further, these two isomeric structures have no structural similarity with the determined C<sub>2v</sub> structure of C<sub>9</sub>H<sub>3</sub>, which is inconsistent with the observation of nearly identical values of the H/D isotopic shift  $\Delta^{III}$  in C<sub>9</sub>H<sub>3</sub> and C<sub>11</sub>H<sub>3</sub>. This leads to the conclusion that the isomeric structure of the observed C<sub>11</sub>H<sub>3</sub> must be H<sup>(I)</sup>C<sub>4</sub>[C(C<sub>2</sub>H<sup>(III)</sup>)]C<sub>4</sub>H<sup>(III)</sup>, as illustrated in Fig. 1(b).

## IV. DISCUSSION

The structural similarities between different unsaturated hydrocarbons can be derived from their H/D isotopic shifts. The H/D isotopic shift in an electronic transition of a polyhydride originates from the change of zero point energy upon electronic excitation,<sup>22</sup> which is related to the difference of the molecular structure in lower and upper state. In both C<sub>9</sub>H<sub>3</sub> and C<sub>11</sub>H<sub>3</sub>, the prominent isotopic shift,  $\Delta^{III}$ , is exactly the same ( $+34.9$  cm<sup>-1</sup>), and this makes it likely that the electronic excitation arises from a mutual substructure H<sup>(I)</sup>C<sub>4</sub>C<sup>\*</sup>C<sub>4</sub>H<sup>(III)</sup>. The near-zero value of  $\Delta^{II}$  indicates that upon electronic excitation there is almost no change in the H<sup>II</sup>-containing substructures of the two molecules. This is confirmed by calculations on the Wiberg bond indices and the active molecular orbitals in C<sub>9</sub>H<sub>3</sub> and C<sub>11</sub>H<sub>3</sub>. The calculations show that the distribution of the conjugated  $\Pi$  bonds in the HC<sub>4</sub>C<sup>\*</sup>C<sub>4</sub>H substructure of the two molecules is almost the same (see Figs. 1 and 5).

The observed origin band positions for C<sub>9</sub>H<sub>3</sub> and C<sub>11</sub>H<sub>3</sub> are close and do not reflect the typical “particle in a one-dimensional box” behaviour, i.e., lower absorption energies

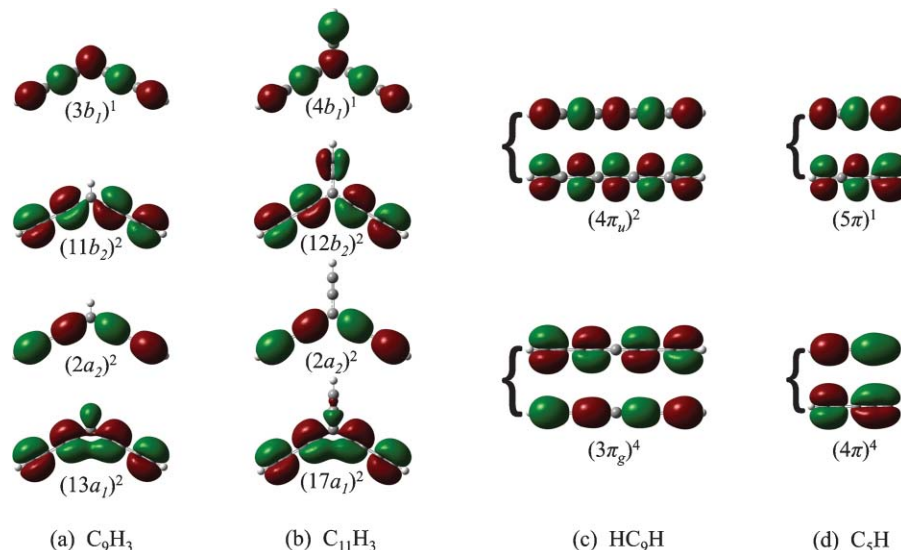


FIG. 5. Panels (a) and (b): calculated active molecular orbitals (MOs) in  $C_9H_3$  and  $C_{11}H_3$ . Panels (c) and (d): calculated active  $\pi$  MOs in the conjugated  $\Pi$  bonds of  $C_5H$  and  $HC_9H$ . The experimental spectra shown in Figs. 2 and 3 arise from the  $a_2 \rightarrow b_1$  electronic excitations from the ground state configurations shown in panels (a) and (b), respectively.

for increasing conjugated chain lengths.<sup>9,23</sup> Indeed, the chain length along the conjugated  $\Pi$  bond does not really increase when adding two C-atoms along the  $C_{2v}$  symmetry axis. In contrast, it is expected that the  $C_7H_3$  radical, with a geometric structure previously determined as a three-membered ring bearing chain, should exhibit rather different H/D isotopic shifts compared to  $C_9H_3$  and  $C_{11}H_3$ . Indeed, the reported H/D isotopic shift for the fully deuterated  $C_7D_3$  is  $\sim +50 \text{ cm}^{-1}$ .<sup>13</sup>

The obtained H/D isotopic shifts can be compared to those of other linear hydrocarbon chains. The isotopic shifts  $\Delta^{I/III}$  ( $\sim +34.9 \text{ cm}^{-1}$ ) of  $C_9H_3$  and  $C_{11}H_3$  is very close to the H/D isotopic shifts of  $C_5H$  ( $\sim +33.8 \text{ cm}^{-1}$  for  $C_5D$ ) and  $HC_9H$  ( $\sim +38.8 \text{ cm}^{-1}$  for  $HC_9D$ ).<sup>24,25</sup> As shown in Fig. 5, the calculated molecular orbitals of the linear  $C_5H$  and  $HC_9H$  indicate that the conjugated  $\Pi$  bonds in the two linear chains are indeed very similar to those in  $C_9H_3$  and  $C_{11}H_3$ . Figure 1 shows that the substructure  $HC_4C^*C_4H$  in  $C_9H_3$  and  $C_{11}H_3$  has the form of two combined  $C_5H$  chains or a bent  $HC_9H$  structure, with a bent angle of  $\sim 120^\circ$  which is very close to the typical bond angle of aromatic rings. To understand these correlations also theoretically, extended CASSCF calculations have been performed on the  $C_9H_3$  and  $HC_9H$  configurations. The result shows that the two pairs of active MOs in  $C_9H_3$ , ( $2a_2$  and  $11b_2$ ) and ( $13a_1$  and  $3b_1$ ), are correlated to the degenerate ( $3\pi_g$ ) and ( $4\pi_u$ ) orbitals in  $HC_9H$ , respectively. Specifically, the former two pairs are split from the latter two  $\pi$  orbitals when the nine-carbon containing chain changes from a linear to a bent conformation. These structural correlations also suggest that nonlinear open chain species have the potential to act as intermediates in the formation of polycyclic aromatic rings in a reactive plasma or combustion flame.

## V. CONCLUSION

In conclusion, the results presented here show that deuterium labeling is a useful approach to characterize the molecular structure of polyhydrogenated carbon chains. Specifically

the structures of  $C_9H_3$  and  $C_{11}H_3$  molecules were determined from their optical spectra. In general, optical spectra of D-substituted species can provide molecular symmetry information of polyhydrides, as well as chemical bond correlations in the substructures containing D-labeled hydrogen. The described method may become more challenging for the D-labeling of a polyhydride with a larger number of hydrogen atoms, because the cumulative variety of isotopologues will likely result in overlapping isotopic bands. In such cases, the isotopic labeling in mass-selective detection schemes, such as REMPI-TOF and ion trap spectroscopy, may provide a useful alternative.

## ACKNOWLEDGMENTS

This work is financially supported by the Netherlands Foundation for Fundamental Research of Matter (FOM) and performed within the context of the Netherlands Astrochemistry Network. Samples of  $C_2D_2$  were generously made available by Professor Schlemmer (University of Cologne).

- <sup>1</sup>K. H. Homann, *Angew. Chem., Int. Ed.* **37**, 2434 (1998).
- <sup>2</sup>H. Ritcher and J. B. Howard, *Prog. Energy Combust. Sci.* **26**, 565 (2000), and references therein.
- <sup>3</sup>T. Fujii and M. Kareev, *J. Appl. Phys.* **89**, 2543 (2001).
- <sup>4</sup>P. Thaddeus, M. C. McCarthy, M. J. Travers, C. A. Gottlieb, and W. Chen, *Faraday Discuss. Chem. Soc.* **109**, 121 (1998).
- <sup>5</sup>H. S. P. Müller, F. Schlöder, J. Stutzki, and G. Winnewisser, *J. Mol. Struct.* **742**, 215 (2005).
- <sup>6</sup>V. Wakelam, I. W. M. Smith, E. Herbst, J. Troe, W. Geppert, H. Linnartz, K. Öberg, E. Roué, M. Agundez, P. Pernot, H. M. Cuppen, J. C. Loison, and D. Talbi, *Space Science Rev.* **156**, 13 (2010).
- <sup>7</sup>M. C. McCarthy and P. Thaddeus, *Chem. Soc. Rev.* **30**, 177 (2001), and references therein.
- <sup>8</sup>A. van Orden and R. J. Saykally, *Chem. Rev.* **98**, 2313 (1998).
- <sup>9</sup>R. Nagarajan and J. P. Maier, *Int. Rev. Phys. Chem.* **29**, 521 (2010), and references therein.
- <sup>10</sup>E. B. Jochnowitz and J. P. Maier, *Annu. Rev. Phys. Chem.* **59**, 519 (2008), and references therein.
- <sup>11</sup>T. W. Schmidt, A. E. Boguslavskiy, T. Pino, H. Ding, and J. P. Maier, *Int. J. Mass. Spectrom.* **228**, 647 (2003).

- <sup>12</sup>T. W. Schmidt, H. Ding, A. E. Boguslavskiy, T. Pino, and J. P. Maier, *J. Phys. Chem. A* **107**, 6550 (2003).
- <sup>13</sup>H. Ding, T. Pino, F. Güthe, and J. P. Maier, *J. Am. Chem. Soc.* **125**, 14626 (2003).
- <sup>14</sup>C. Zhang, *J. Chem. Phys.* **121**, 8212 (2004).
- <sup>15</sup>D. Zhao, N. Wehres, H. Linnartz, and W. Ubachs, *Chem. Phys. Lett.* **501**, 232 (2011).
- <sup>16</sup>H. Linnartz in *Cavity Ring-Down Spectroscopy – Techniques and Applications*, edited by G. Berden and R. Engeln (Wiley-Blackwell, Chichester, United Kingdom, 2009), pp. 145–179.
- <sup>17</sup>A. D. Becke, *J. Chem. Phys.* **98**, 5648 (1993).
- <sup>18</sup>F. Bernardi, A. Bottini, J. J. W. McDougall, M. A. Robb, and H. B. Schlegel, *Faraday Symp. Chem. Soc.* **19**, 137 (1984).
- <sup>19</sup>M. J. Frisch, G. W. Trucks, H. B. Schlegel, G. E. Scuseria *et al.*, GAUSSIAN 03, Revision B.04, Gaussian, Inc., Pittsburgh, PA, 2003.
- <sup>20</sup>H. Linnartz, T. Motylewski, O. Väizert, J. P. Maier, A. J. Apponi, M. C. McCarthy, C. A. Gottlieb, and P. Thaddeus, *J. Mol. Spectrosc.* **197**, 1 (1999).
- <sup>21</sup>M. P. Andersson and P. Uvdal, *J. Phys. Chem. A* **109**, 2937 (2005).
- <sup>22</sup>G. Herzberg, *Molecular Spectra and Molecular Structure III. Electronic Spectra and Electronic Structure of Polyatomic Molecules* (D. Van Nostrand, New York, 1966), pp. 181–183.
- <sup>23</sup>J. P. Maier, *Chem. Soc. Rev.* **26**, 21 (1997).
- <sup>24</sup>H. Ding, T. Pino, F. Guthe, and J. P. Maier, *J. Chem. Phys.* **117**, 8362 (2002).
- <sup>25</sup>C. D. Ball, M. C. McCarthy, and P. Thaddeus, *Astrophys. J.* **523**, L89 (1999).